

A SEARCH FOR THE HIGGS BOSON PRODUCED IN ASSOCIATION WITH TOP QUARKS IN MULTILEPTON FINAL STATES AT ATLAS

Chris Lester

A DISSERTATION
in
Physics and Astronomy

Presented to the Faculties of The University of Pennsylvania
in Partial Fulfillment of the Requirements for the Degree of Doctor of Philosophy
2014

Joseph Kroll, Professor, Physics
Supervisor of Dissertation

A.T. Charlie Johnson, Professor, Physics
Graduate Group Chairperson

Dissertation Committee

Randall Kamien, Professor, Physics

I. Joseph Kroll, Professor, Physics

Elliot Lipeles, Assistant Professor, Physics

Burt Ovrut, Professor, Physics

Joseph Kroll, Professor, Physics

A SEARCH FOR THE HIGGS BOSON PRODUCED IN ASSOCIATION WITH TOP QUARKS IN MULTILEPTON FINAL STATES AT ATLAS

COPYRIGHT
2014
Chris Lester

All rights reserved.

Acknowledgements

30 Acknowledgements acknowledgements acknowledgements acknowledgements acknowledgements ac-
31 knowledgements acknowledgements acknowledgements acknowledgements acknowledgements acknowl-
32 edgements acknowledgements acknowledgements acknowledgements acknowledgements acknowledgements
33 acknowledgements acknowledgements acknowledgements acknowledgements acknowledgements acknowledgements
34 acknowledgements acknowledgements acknowledgements acknowledgements acknowledgements acknowledgements
35 acknowledgements acknowledgements.

36 Acknowledgements acknowledgements acknowledgements acknowledgements acknowledgements ac-
37 knowledgements acknowledgements acknowledgements acknowledgements acknowledgements acknowledgements
38 acknowledgements acknowledgements acknowledgements acknowledgements acknowledgements acknowledgements
39 acknowledgements acknowledgements acknowledgements acknowledgements acknowledgements acknowledgements
40 acknowledgements acknowledgements acknowledgements acknowledgements acknowledgements acknowledgements
41 acknowledgements acknowledgements.

42 Acknowledgements acknowledgements acknowledgements acknowledgements acknowledgements ac-
43 knowledgements acknowledgements acknowledgements acknowledgements acknowledgements acknowledgements
44 acknowledgements acknowledgements acknowledgements acknowledgements acknowledgements acknowledgements
45 acknowledgements acknowledgements acknowledgements acknowledgements acknowledgements acknowledgements
46 acknowledgements acknowledgements acknowledgements acknowledgements acknowledgements acknowledgements
47 acknowledgements acknowledgements.

ABSTRACT

A SEARCH FOR THE HIGGS BOSON PRODUCED IN ASSOCIATION WITH TOP
50 QUARKS IN MULTILEPTON FINAL STATES AT ATLAS

Chris Lester

Joseph Kroll

Abstract abstract abstract abstract abstract abstract abstract abstract abstract
54 abstract abstract abstract abstract abstract abstract abstract abstract abstract
55 abstract abstract abstract abstract abstract abstract abstract abstract abstract
56 abstract abstract abstract abstract abstract abstract abstract abstract abstract
57 abstract abstract abstract abstract abstract abstract abstract abstract abstract
58 abstract abstract abstract abstract abstract abstract abstract abstract abstract
59 abstract abstract abstract abstract abstract abstract abstract abstract abstract
60 abstract abstract abstract abstract abstract abstract abstract abstract abstract
61 abstract abstract abstract abstract abstract abstract abstract abstract abstract.

Contents

63	Acknowledgements	iii
64	Abstract	iv
65	Contents	v
66	Preface	vii
67	1 Introduction	1
68	2 Theoretical Background	2
69	2.1 The Standard Model	2
70	2.1.1 The Standard Model Structure	2
71	2.1.2 Electroweak Symmetry Breaking and the Higgs	3
72	2.1.3 The Standard Model Parameters	4
73	2.2 Collider Physics and the Higgs	4
74	2.2.1 Higgs Discovery at the LHC	7
75	2.2.2 $t\bar{t}H$ Production	8
76	2.3 Conclusion	10
77	3 The Large Hadron Collider	11
78	3.1 The Large Hadron Collider	11
79	3.1.1 The Accelerator Complex	11
80	3.1.2 Beam Parameters and Collisions	12
81	3.2 The 2012 Dataset	13

82	4 The ATLAS Experiment	15
83	4.1 Data	17
84	4.2 Simulation	17
85	5 Electrons	18
86	5.1 Electrons at Hadron Colliders	18
87	5.2 Reconstruction of Electron at ATLAS	18
88	5.3 Identification of Electrons at ATLAS	18
89	5.3.1 Pile-up	18
90	5.3.2 Trigger vs. Offline	18
91	5.3.3 2011 Menu	18
92	5.3.4 2012 Menu	18
93	5.3.5 Electron Likelihood	18
94	5.4 Measurement of Electron Efficiency at ATLAS	18
95	5.4.1 Techniques	18
96	5.4.2 Issues	18
97	6 Search for the TTH Decay in the Multilepton Channel	19
98	6.1 Introduction	19
99	6.2 Event Selection	19
100	6.3 Optimization	19
101	6.4 Background Measurements	19
102	6.5 Systematic Assessment	19
103	6.6 Results	19
104	6.7 Combination	19
105	7 Conclusions	20
106	7.1 Higgs Results in Review	20
107	7.2 Prospects for Future	20
108	Bibliography	21

Preface

110 This is the preface. Blah blah blah blah blah blah. Blah blah blah blah blah blah. Blah
111 blah blah blah blah blah blah. Blah blah blah blah blah blah. Blah blah blah blah blah blah
112 blah. Blah blah blah blah blah blah. Blah blah blah blah blah blah. Blah blah blah blah
113 blah blah blah. Blah blah blah blah blah blah. Blah blah blah blah blah blah. Blah blah
114 blah blah blah blah. Blah blah blah blah blah blah. Blah blah blah blah blah blah.
115 Blah blah blah blah blah. Blah blah blah blah blah.

116 Blah blah blah blah blah blah. Blah blah blah blah blah blah. Blah blah blah blah
117 blah. Blah blah blah blah blah blah. Blah blah blah blah blah blah. Blah blah blah
118 blah blah blah. Blah blah blah blah blah blah. Blah blah blah blah blah blah. Blah
119 blah blah blah blah blah. Blah blah blah blah blah blah. Blah blah blah blah blah
120 blah. Blah blah blah blah blah blah. Blah blah blah blah blah blah. Blah blah blah
121 blah blah.

Chris Lester
CERN, Fall 2014

¹²³

CHAPTER 1

¹²⁴

Introduction

¹²⁵ Here is a citation [?].

126

CHAPTER 2

127

Theoretical Background

128 The Standard Model of particle physics (SM) is an extraordinarily successful description of the funda-
129 mental constituents of matter and their interactions. Experiments over the past 50 years have verified
130 the extremely precise prediction of the SM. This success has culminated most recently in the discovery
131 of the Higgs Boson. This chapter provides a brief introduction to the structure of the SM and how
132 scientists are able to test it using hadron collider but focuses primarily on the physics of the Higgs
133 boson and its decays to top quarks. Particular attention is given to the importance of a measurement
134 of the rate at which Higgs Bosons are produced in association of top quarks in the context of testing
135 the predictions the SM.

136 **2.1 The Standard Model**

137 **2.1.1 The Standard Model Structure**

138 The Standard Model (SM) [1, 2, 3, 4] is an example of a quantum field theory that describes the
139 interactions of all of the known fundamental particles. Particles are understood to be excitations of
140 the more fundamental object of the theory, the field. The dynamics and interactions of the fields are
141 derived from the Standard Model Lagrangian, which is constructed to be symmetric under transfor-
142 mations of the group $SU(3) \times SU(2) \times U(1)$. $SU(3)$ is the group for the color, $SU(2)$ is the group for
143 weak iso spin, and $U(1)$ is the group for weak hyper-charge.

144 Gauging the symmetries demands the introduction of 8 massless gluons, or the boson (full integer
145 spin) carriers of the strong force [5] from the generators $SU(3)$ symmetry, and the 4 massless bosons,
146 carriers for the weak and electromagnetic forces from the 3 generators of the $SU(2)$ and 1 generator
147 of the $U(1)$ group. The weak and the electromagnetic forces are considered part of a larger single

148 unified electroweak group $SU(2) \times U(1)$ and the associated generators mix.

149 The gauge symmetry allows the theory to be re-normalizable [6], meaning that unwanted infinities
150 can be absorbed into observables from theory in a way that allows the theory to be able to predict
151 physics at multiple energy scales. Singlets of the $SU(3)$ group are fermions (half-integer spin particles)
152 called leptons and do not interact with the strong, whereas doublets of the $SU(3)$ group are called
153 quarks and do interact with the strong force. The SM is a chiral theory: the weak force violates parity,
154 as it only couples to left-chiral particles or right-chiral antiparticles. This means that right-chiral and
155 left-chiral fermions arise from different fields, which are different representations of the weak isospin
156 group.

157 The discovery of particles and new interactions in various experiments is intertwined with the
158 development of the theory that spans many decades and is not discussed in detail here.

159 So far, 3 separate generations of both quarks and leptons have been discovered, differing only by
160 mass. The gluon and the 4 electroweak bosons have also been discovered (W^+ , W^- , Z^0 , and γ) ¹. The
161 reason for this 3-fold replication is not known.

162 2.1.2 Electroweak Symmetry Breaking and the Higgs

163 Despite the simple structure of theory, the discovery of massive fundamental particles creates two sets
164 of problems both related to $SU(2) \times U(1)$. First, the force-carrying bosons must enter the theory
165 without mass or the symmetries will be explicitly broken in the Lagrangian. Second, adding fermion
166 masses to theory in an ad-hoc way allows the right-chiral and left-chiral fermions to mix. Since they
167 possess different quantum numbers, as different representations of the weak-isospin group, this too
168 breaks gauge invariance.

169 To solve these problems, spontaneous electro-weak symmetry breaking (EWSB) is introduced via
170 the Brout-Englert-Higgs mechanism [7, 8, 9]. A massive scalar field in an electro-weak doublet is
171 added to the theory with 4 new degrees of freedom and a potential which includes a quartic self-
172 interaction term. Each fermion field interacts with the scalar field via a different Yukawa coupling,
173 which unites the left and right chiral fields of a single particle type. This field explicitly preserves all
174 of the symmetries, but the minimum of the potential does not occur when the expectation of the field
175 is zero. The field eventually falls to a state, where it acquires a vacuum-expectation value. However,
176 a non-zero field must therefore point in a particular direction of weak-isospin space, breaking the
177 symmetry.

1The actual particles observed to be produced and propagate may be linear combinations of the underlying generators (for the bosons) or gauge representations (for the fermions).

178 The consequences of this spontaneous symmetry breaking are tremendous. First, the universe
 179 is filled with a field with a non-zero expectation value. The theory can be expanded around this
 180 new value and 3 of the degrees of freedom can be interpreted as the longitudinal polarizations of
 181 the W^+ , W^- , and Z^0 , while the 4th remains a scalar field, called the Higgs field with an associated
 182 particle called the Higgs particle or "Higgs" The weak bosons acquire a mass via their longitudinal
 183 polarizations and the Yukawa couplings of the scalar field to the fermions now behave like a mass
 184 term at the this new minimum.

185 2.1.3 The Standard Model Parameters

186 Although the SM structure is set by specifying the gauge groups, the EWSB mechanism, and ac-
 187 knowledging the 3-fold replication of the fermions, confronting the SM with experiment requires the
 188 measurement of 17² free parameters, which are unconstrained from the theory. These free parameters
 189 include the fermion masses (from the Yukawa coupling), the force coupling constants, the angles and
 190 phase of the mixing between quarks, and constants from the Higgs and electroweak sector³.

191 Experiments have provided a number of measurements of the parameters of the SM[10]. Prior
 192 to the discovery of the Higgs boson (discussed later) the Higgs mass, however, was the only fully
 193 unconstrained parameter, although its value could be inferred via its involvement in loop corrections
 194 on the top mass (M_t) and the W mass (M_W). The GFitter collaboration assembles all relevant
 195 electroweak observable measurements into a statistical model and then allows certain measurements to
 196 float within their uncertainty to allow for a fit among multiple correlated measurements measurements
 197 [11]. Figure 2.1 shows the fitted constraints on 4 key SM parameters (M_H , M_W , M_t , $\sin^2\theta_w$) with
 198 actual measurements overlaid. The addition to the fit of the measured Higgs mass from the ATLAS
 199 and CMS collaborations creates a small tension, as the other observables prefer the mass to be much
 200 lower (~ 80 GeV/ c^2). The tension in the combined electroweak fit (including the Higgs) is not
 201 statistically significant with a p -value of 0.07.

202 2.2 Collider Physics and the Higgs

203 To test the theory, physicists accelerate particles to extremely high energies and force them to interact
 204 through collisions. Typically, the particles accelerated are electrons or protons, since they are stable.

²There are additional parameters from neutrino mass terms and mixing but it is unclear how to include these into the Standard Model, since it does not predict right-chiral neutrinos

³ The electroweak sector includes parameters like mass of the W^\pm and Z^0 bosons, the weak mixing angle, $\sin^2\theta_w$, the fermi constant G_F , and Higgs Mass and vacuum expectation value. These parameters however are not wholly independent. As discussed above, it is only necessary theoretically to specify the two parameters relevant to the Higgs potential and the two coupling associated with the gauge groups

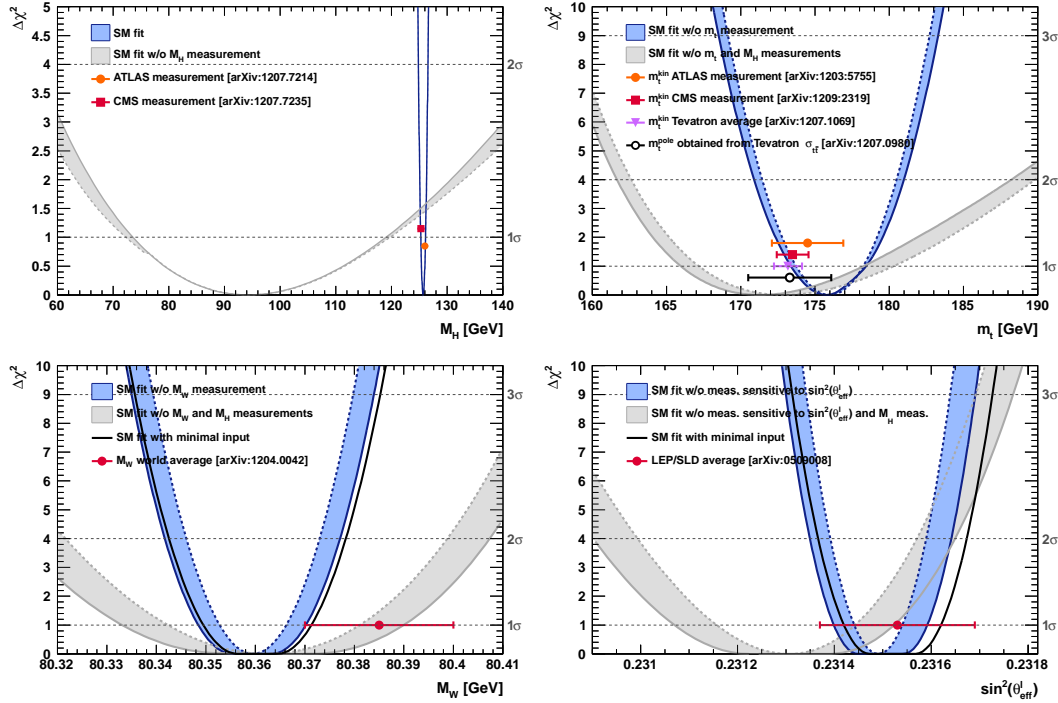


Figure 2.1: χ^2 as a function of the Higgs mass (top left), the top quark mass (top right), the W boson mass (bottom left) and the effective weak mixing angle (bottom right) for the combined SM fit from the GFitter group. The data points placed along $\chi^2 = 1$ represent direct measurements of the respective observable and their $\pm 1\sigma$ uncertainties. The grey (blue) bands show the results when excluding (including) the new M_H measurements from (in) the fits.

205 Electron-positron collider machines have a rich history of discovery and measurement in particle
 206 physics. The advantage of electron accelerators is that the colliding element is itself a fundamental
 207 particle. However, due synchrotron radiation, curvature of the beam line becomes problematic for
 208 high energy beams. Hadron colliders, specifically, proton-proton and proton-anti-proton colliders can
 209 be accelerated in rings without large losses due to synchrotron radiation, but the actual colliding
 210 objects at high energies are the constituent quarks and gluons. This complicates analysis because the
 211 initial state of the system is not discernible on a per-collision basis and momentum of hard scatter
 212 system is unknown along the beam direction.

213 Collider physics rely on form-factor descriptions of the colliding hadrons that describe the fraction
 214 of momentum carried by the hadrons constituent 'partons'. These are called parton-distribution
 215 functions, seen in Figure 2.2, and are factorized and integrated through the theoretical calculations
 216 of various collision processes [12].

217 At the Large Hadron Collider or LHC (discussed in detail in Chapter 3 a proton-proton colluder,

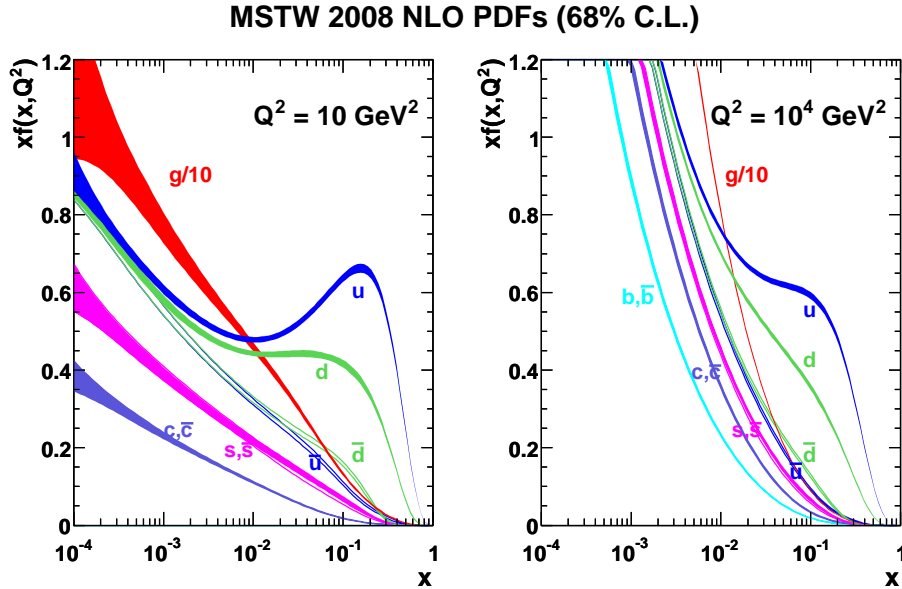


Figure 2.2: Proton Parton Distribution Functions (PDFs) form the MSTW Collaboration at $Q^2 = 10 \text{ GeV}^2$ and $Q^2 = 10^4 \text{ GeV}^2$

the types of initial states are quark-quark, quark-gluon, and gluon-gluon. Gluon collisions dominate overall, due to the large number of gluons inside the proton, though the relative importance of different initial states changes with the energy scale of the collision and the type of final state sought after.

A prime motivation for the construction of the Large Hadron Collider was the discovery or exclusion of the Higgs boson[13]. LEP and the Tevatron excluded large swaths of possible Higgs boson masses, especially below $114 \text{ GeV}/c^2$ and the unitarity of certain diagrams including the $WWWW$ vertex required the mass to be below about 1 TeV, a range that was achievable at the LHC with high luminosity running [10].

Despite the ubiquity of Higgs couplings, Higgs boson production at the LHC is a low rate process. Because it couples to fermions proportional to mass and because the colliding particles must be stable and therefore light, production of the Higgs must occur through virtual states.

The Higgs boson can be produced through collision at the LHC via 4 mechanisms: gluon-fusion (ggF), vector-boson fusion (VBF), Higgsstrahlung (VH), and production in association with top quarks ($t\bar{t}H$). The diagrams are shown in Figure 2.3 and the production cross-sections as a function of Higgs mass for the 8 TeV LHC proton-proton running are shown in Figure 2.4 [14]. The largest production cross-section is via the gluon fusion channel at 20 pb, which proceeds through a fermion loop that is dominated by the top quark, because of its large Yukawa coupling to the Higgs.

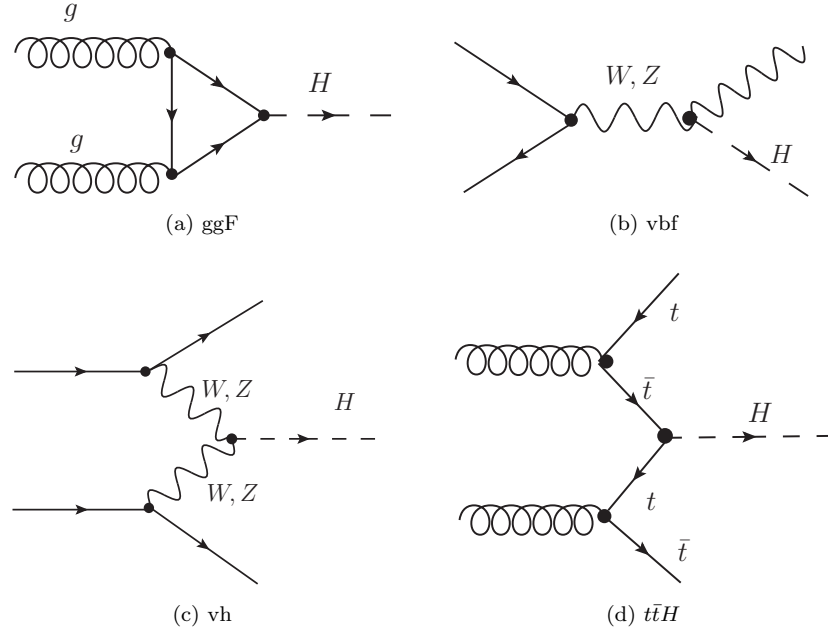


Figure 2.3: Dominant Higgs production modes at the LHC

Because the Higgs' couples to every massive particle, it has a rich set of decays also seen in Figure 2.4, especially for $m_H = 125$. Studies of Higgs properties at hadron colliders offers many tests of the Standard Model and ample room for searches for new physics. These tests specifically can verify the link between Yukawa coupling and the particles mass and further constrain details of EWSB by examining Higgs coupling to the weak bosons.

2.2.1 Higgs Discovery at the LHC

In 2012 both ATLAS and CMS announced the discovery of a new boson consistent with the Higgs by examining the results of Higgs searches in a number of decay channels ($H \rightarrow W^+W^-$, $H \rightarrow Z^0Z^0$, and $H \rightarrow \gamma\gamma$) in the 2011 dataset at $\sqrt{s} = 7$ TeV and part of the 2012 dataset at $\sqrt{s} = 8$ TeV. By 2013 and 2014, both experiments have updated and/or finalized their results for the full 2011 and 2012 datasets [15, 16]. I will focus on the ATLAS results in the following. The ATLAS measurements constrain both the Higgs mass[17] and spin[18], as well as provide constraints to the Higgs couplings to different particles.

Figure 2.5 show the results of the searches in all of the measurement channels as well as constraints on the SM Higgs coupling parameters in an example fit, where the couplings to the top-quark, bottom-

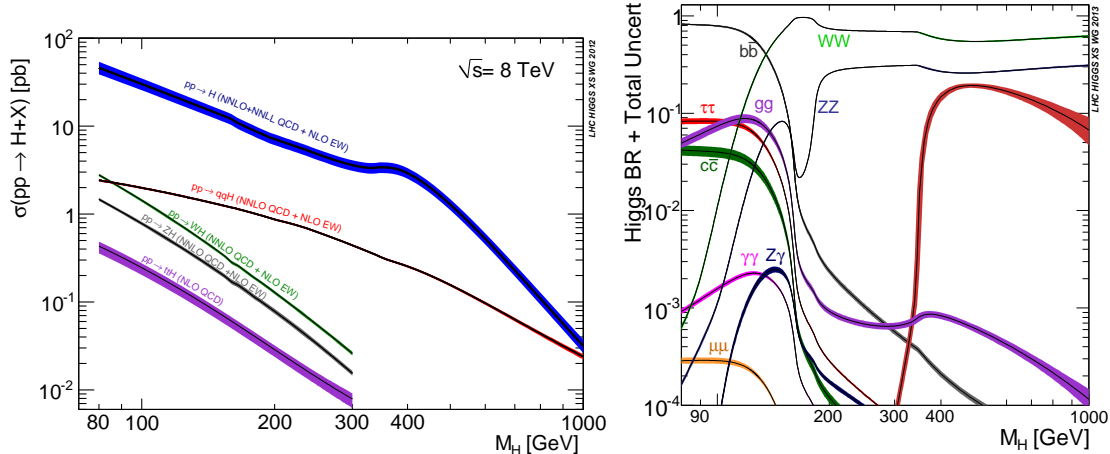


Figure 2.4: 8 TeV LHC Higgs production cross-sections (left) and decay branching fractions

quark, W,Z, and τ are allowed to fluctuate independently. These rely on measurements binned in different production and decay channels. They are dominated by higher statistics results in the gluon-fusion production modes, but measurements in the VH and VBF modes are close to SM sensitivity.

The combined results show basic agreement with the SM with much room for improvement with the addition of new production and decay modes and higher statistics. The coupling constraints are particularly strong for the W and Z, which are the most sensitive decay channels, and top quark due to the dominance of the top Yukawa in the ggF loop.

2.2.2 $t\bar{t}H$ Production

Notably absent thus far in the SM are searches for the Higgs in the $t\bar{t}H$ production channel, due to the lack of statistics. Searches are underway and initial results are close to SM sensitivity for ATLAS and CMS. More will be discussed about particular searches later. $t\bar{t}H$ production depends on the top Yukawa coupling at tree level. Comparison of the gluon-fusion and the $t\bar{t}H$ modes would allow for disentangling the effects of new particles in the gluon-fusion loop[19]. For instance, generic models would allow for the introduction of new colored particles into the loop. The simplest of these models would be the addition of a new generation of quarks. Fourth generation quarks, which obtain mass from a Higgs Yukawa coupling are already largely excluded due to their enormous effects on the Higgs production cross-section[20]. Other exotic scenarios allow for new colored particles in the gluon-fusion loop, which are not entirely constrained by present measurements[21, 22, 23]. These include, for instance, Supersymmetric models involving the stop quark.

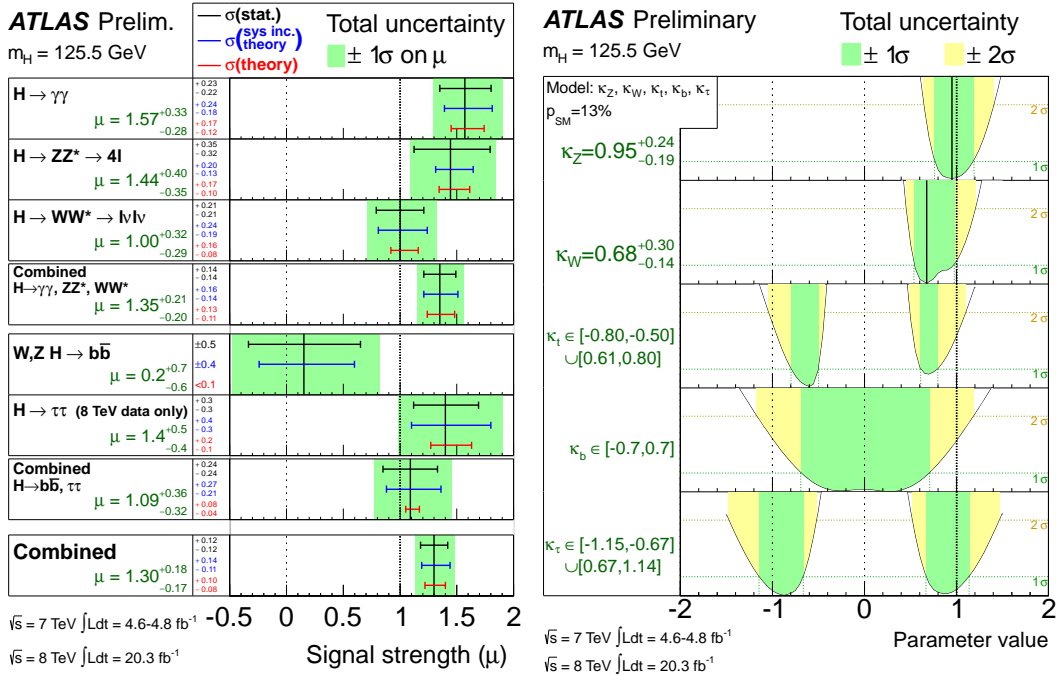


Figure 2.5: ATLAS Higgs combination results for all SM measurement channels as ratios of the measured to SM production cross-sections (left) and extracted Higgs coupling constraint scale-factors for a combined fit to the measurement channels, where the W, Z , top-quark, b -quark, and τ couplings are allowed to float. The p-value of this particular model is 0.13 and in agreement with SM expectations

269 Aside from the loop effects, measurement of the $t\bar{t}H$ production cross-section would provide a
 270 precise measurement of the top Yukawa coupling. When compared with the measured top quark mass,
 271 this tests the Higgs mass generation properties for up-type quarks. Despite similar uncertainties on
 272 the overall production cross-sections for $t\bar{t}H$ and the gluon-fusion modes, both of which depend on the
 273 top Yukawa, most of these uncertainties would cancel for $t\bar{t}H$ if normalized to the topologically similar
 274 $t\bar{t}Z$. Finally, the uniqueness of the experimental signature means that searches for $t\bar{t}$ signatures can
 275 be performed for a variety of Higgs decays ($\gamma\gamma, b\bar{b}, WW, ZZ$, and $\tau\bar{\tau}$ with roughly similar degrees of
 276 sensitivity (within a factor of 10)[19].

277 It is important to note the importance of the top Yukawa coupling to the overall structure of the
 278 SM, due to its enormous size compared to other couplings. The top Yukawa is for instance 350000x as
 279 large as the electron Yukawa coupling. Because of this the top Yukawa coupling, along with the Higgs
 280 mass, is one of the most important pieces of the renormalization group equations (RGE) responsible
 281 for the running of the parameter that determines the Higgs self-coupling λ . If this parameter runs
 282 negative, then the potential responsible for the entire mechanism of EWSB no longer has a minimum
 283 and becomes unbounded, resulting in instability in the universe [24]. Metastability occurs when the

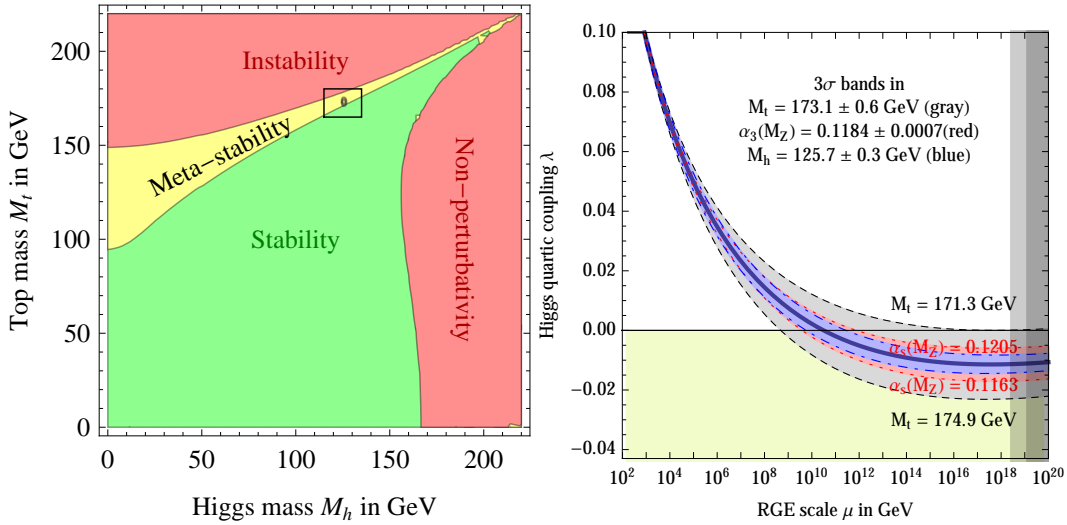


Figure 2.6: RGE for the running of the SM parameter, λ for the Higgs self-coupling term with present values and uncertainty bands for M_H and M_t (left). The two-dimensional plot colored (right) shows regions for which the SM is stable, unstable and metastable based on this RGE

shape of the potential allows for a false local minimum. Figure 2.6 shows the running of this parameter, the regions for which the universe is stable, unstable and metastable. Current measurements suggest that universe lies in a metastable island⁴.

2.3 Conclusion

The Standard Model, despite its success in providing a unified description of fundamental particles and interactions into single theory, has its flaws. These have been discussed in depth elsewhere, but include issues like the description of massive neutrinos, the failure to include gravity, and the unnaturalness of large quantum corrections to Higgs parameters. For these reasons, it seems the SM might be a lower energy approximation to a more fundamental theory. The discovery of the Higgs boson at the LHC provided a stunning verification of one of the fundamental aspects of the theory but at the same time offers new area to search for glimpses of something grander. The production of samples of Higgs bosons allows for a rich array of new tests of the Standard Model, which is now finally over-constrained by experiment. Searches for the $t\bar{t}H$ production, one category of which is the topic of this thesis, provide tree-level access to a central parameter of the theory, the top Yukawa coupling, as well as access a variety of Higgs decays, which will eventually provide a rigorous new test of the SM.

⁴The RGE assumed that there is no new physics at all energy scales

300

CHAPTER 3

301

The Large Hadron Collider

302 Production of a sufficient number of high energy collisions to adequately explore particle physics at
303 the electro-weak scale required the development of one of the most complex machines ever built,
304 the Large Hadron Collider or LHC. This chapter provides a very brief overview of the machine with
305 particular focus on the 2012 dataset of proton-proton collisions it enabled. The technology involved in
306 the development of the LHC and very briefly touched upon in this chapter is an enormous achievement
307 in its own right and is documented in detail here [25, 26, 27].

308 **3.1 The Large Hadron Collider**

309 The Large Hadron Collider(LHC) is the world's highest energy particle acclerator and is located
310 100m underneath the Franco-Swiss border at the European Organization for Nuclear Research (CERN)
311 in a 26.7 km tunnel.

312 The LHC is a ciruclar machine capable of accelerating beams of protons and colliding them at
313 center of mass energies up to $\sqrt{s} = 14TeV$ at 4 collision sites around the ring, where 4 experiments are
314 housed (ATLAS[28], CMS[?], LHCb[29], and ALICE[?]). Figure 3.1 is a diagram of the layout of the
315 LHC and its experiments[30]. The LHC also operates in a modes with beams of heavy ions. The LHC
316 is composed of thousands of super-conducting Niobium-Titanium magnets, cooled to $2.7^\circ C$ with
317 liquid Helium, which steer and focus the particle beams, and a superconducting resonant-frequency
318 (RF) cavity,which boosts the beam to higher energies.

319 **3.1.1 The Accelerator Complex**

320 The accelerator complex is a progressive series of machineswith the LHC as the final stage. Protons are
321 obtained from hydrogen atoms and are accelerated to 50 MeV using the Linac2, before being injected

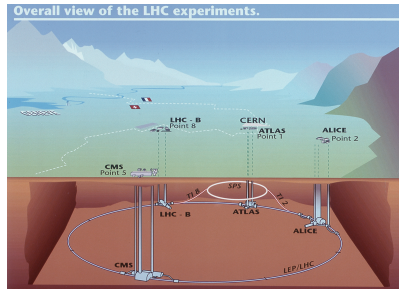


Figure 3.1: Diagram of the Large Hadron collider and location of the 4 main experiments (ATLAS, CMS, LHCb, and ALICE). Around the ring. The diagram also shows the location of the SPS, the final booster ring the accelerator complex that accelerates the protons to 450 GeV before injection into the LHC.

322 into the Proton-Synchrotron Booster (PSB). In the PSB the protons are accelerated to energies of 1.4
 323 GeV for injection in to the Proton-Synchrotron (PS). The PS accelerates the protons to 25 GeV and
 324 dumps bunches into the Super Proton Synchrotron (SPS), where they are accelerated to 450 GeV
 325 and finally dumped into the LHC.

326 3.1.2 Beam Parameters and Collisions

327 For the physics studied at the ATLAS experiment, the two most important parameters of the collisions
 328 provided by the LHC are the center of mass energy and instantaneous luminosity. High center of mass
 329 energies are necessary for the production of new high mass particles, and because the constituents of
 330 the actual collisions are the partons of the proton, the CME of the collisions must in general be much
 331 higher than the mass of the particles needed to be produced. The

332 The instantaneous luminosity of the collisions, \mathcal{L} , is a measure of the collision rate. The integrated
 333 luminosity over time is a measure of the size of the dataset and when multiplied by the cross-section of a
 334 particular process gives the total number of expected events produced for that process. Instantaneous
 335 luminosity depends on the number of colliding bunches of protons, the intensity of those bunches, the
 336 revolution frequency, and the normalized transverse spread of the beam in momentum and position
 337 phase space, called the emittance, and the transverse beam size. The LHC has the option for colliding
 338 beams with 2808 bunches of protons, each with around 10^{11} protons, at a rate of one bunch collision

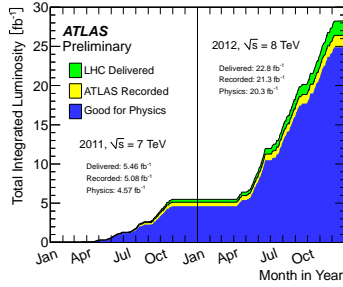


Figure 3.2: Plot showing the accumulation of the integrated luminosity delivered to the ATLAS experiment over 2011 and 2012. The rough size of the usable, physics ready dataset for 2012 is 20 fb^{-1} and is the dataset used for the following analysis.

339 every 25 ns, or 40 MHz. These correspond to a design luminosity of around $10^{34} \text{ cm}^2 \text{ s}^{-1}$ or $10 \text{ nb}^{-1} \text{ s}^{-1}$

341 3.2 The 2012 Dataset

342 The LHC successfully produced datasets for physics studies in 2010, 2011 and 2012. The 2012 proton-
 343 proton dataset was delivered with collisions with a CME of 8 TeV with bunch collisions every 50 ns and
 344 reached a total integrated luminosity of around 20 fb^{-1} [31]. Figure 3.2 shows the accumulation of this
 345 dataset over time. The full LHC design energy was never reached due to worries about faulty dipole
 346 connections involved in the unexpected quenching of the magnets in 2008. Despite doubling the bunch
 347 spacing (thereby halving the bunch collision frequency), the luminosity neared the design luminosity
 348 due to unexpected improvements in the transverse beam profile [32]. This increased the amount of
 349 pile-up, or number of collisions per bunch crossing and in general collision events were busier due to
 350 these multiple interactions]. Figure 3.3 shows the average number of interaction per bunch crossing
 351 for the 2011 and 2012 datasets. The 2012 dataset shows an average of 20-25 interactions.

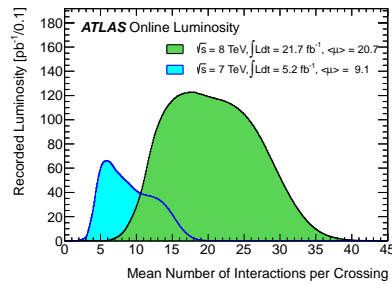


Figure 3.3: The average number of interactions per bunch-crossing for the 2012 and 2011 LHC proton-proton dataset. Most of these interactions are uninteresting but leave energetic signatures in particle detectors called pile-up which interfere with measurements

CHAPTER 4

The ATLAS Experiment

Process	Yield
mm – $j=3$ jets	
Prompts Same-Sign	
$t\bar{t}V, tV$	10.0034 ± 0.26879
$V\gamma$	0.0609 ± 0.44731
VV	6.28008 ± 0.54131
Fake Same-Sign	
$V+jets$	1.22145 ± 117.871
$t\bar{t}$	13.9238 ± 2.01397
top prompts	0 ± 0
single top	1.43354 ± 0.40598
QMisID (DD)	0 ± 0
Data	44

Process	Yield
$m/m - i=3$ jets	
Prompts Same-Sign	
$t\bar{t}V, tV$	0.73613 ± 0.06453
$V\gamma$	4.84582 ± 3.98757
VV	4.3491 ± 2.1029
Fake Same-Sign	
$V+jets$	21.7726 ± 117.962
$t\bar{t}$	114.944 ± 5.36963
top prompts	0 ± 0
single top	77.7706 ± 3.06867
QMisID (DD)	0 ± 0
Data	249

Process	Yield
$m/m - 4$ jets	
Prompts Same-Sign	
$t\bar{t}V, tV$	0.25381 ± 0.03374
$V\gamma$	0.02117 ± 3.95125
VV	0.11317 ± 1.98304
Fake Same-Sign	
$V+jets$	0.1074 ± 117.871
$t\bar{t}$	27.9196 ± 2.61014
top prompts	0 ± 0
single top	2.33972 ± 0.49333
QMisID (DD)	0 ± 0
Data	21

355

356

Process	Yield
m/m – 5 jets	
Prompts Same-Sign	
$t\bar{t}V, tV$	0.29783 ± 0.03896
$V\gamma$	0 ± 0
VV	0.00186 ± 1.98248
Fake Same-Sign	
$V+jets$	0 ± 0
$t\bar{t}$	14.4522 ± 1.842
top prompts	0 ± 0
single top	0.15287 ± 0.11273
QMisID (DD)	0 ± 0
Data	11

357

358 4.1 Data

359 4.2 Simulation

360

CHAPTER 5

361

Electrons

362 **5.1 Electrons at Hadron Colliders**

363 **5.2 Reconstruction of Electron at ATLAS**

364 **5.3 Identification of Electrons at ATLAS**

365 **5.3.1 Pile-up**

366 **5.3.2 Trigger vs. Offline**

367 **5.3.3 2011 Menu**

368 **5.3.4 2012 Menu**

369 **5.3.5 Electron Likelihood**

370 **5.4 Measurement of Electron Efficiency at ATLAS**

371 **5.4.1 Techniques**

372 **5.4.2 Issues**

373

CHAPTER 6

374

Search for the TTH Decay in the Multilepton Channel

375

376 **6.1 Introduction**

377 **6.2 Event Selection**

378 **6.3 Optimization**

379 **6.4 Background Measurements**

380 **6.5 Systematic Assessment**

381 **6.6 Results**

382 **6.7 Combination**

383

CHAPTER 7

384

Conclusions

385 **7.1 Higgs Results in Review**

386 **7.2 Prospects for Future**

Bibliography

- 388 [1] S. L. Glashow, *Partial-symmetries of weak interactions*, Nucl. Phys. **22** (1961) no. 4, 579. [2.1.1](#)
- 389 [2] S. Weinberg, *A Model of Leptons*, Phys. Rev. Lett. **19** (1967) 1264. [2.1.1](#)
- 390 [3] A. Salam and J. C. Ward, *Gauge theory of elementary interactions*, Phys. Rev. **136** (1964)
391 [763–768](#). [2.1.1](#)
- 392 [4] S. Weinberg, *Non-abelian gauge theories of the strong interactions*, Phys. Rev. Lett. **31** (1973)
393 [494–497](#). [2.1.1](#)
- 394 [5] D. J. Gross and F. Wilczek, *Ultraviolet behavior of non-abelian gauge theories*, Phys. Rev. Lett.
395 **30** (1973) 1343–1346. [2.1.1](#)
- 396 [6] G. 't Hooft and M. Veltman, *Regularization and renormalization of gauge fields*, Nuclear
397 Physics B **44** (1972) 189 – 213. [2.1.1](#)
- 398 [7] P. W. Higgs, *Broken symmetries and the masses of gauge bosons*, Phys. Rev. Lett. **13** (1964)
399 [508](#). [2.1.2](#)
- 400 [8] P. W. Higgs, *Spontaneous symmetry breakdown without massless bosons*, Phys. Rev. **145** (1966)
401 [1156](#). [2.1.2](#)
- 402 [9] F. Englert and R. Brout, *Broken Symmetry and the Mass of Gauge Vector Mesons*,
403 Phys. Rev. Lett. **13** (1964) 321–322. [2.1.2](#)
- 404 [10] The ALEPH, CDF, DØ, DELPHI, L3, OPAL, SLD Collaborations, the LEP Electroweak
405 Working Group, the Tevatron Electroweak Working Group, and the SLD electroweak and
406 heavy flavour groups, *Precision Electroweak Measurements and Constraints on the Standard
407 Model*, CERN-PH-EP-2010-095 (2010) , [arXiv:1012.2367 \[hep-ex\]](#). [2.1.3](#), [2.2](#)
- 408 [11] M. Baak, M. Goebel, J. Haller, A. Hoecker, D. Kennedy, R. Kogler, K. Mnig, M. Schott, and
409 J. Stelzer, *The electroweak fit of the standard model after the discovery of a new boson at the
410 LHC*, The European Physical Journal C **72** (2012) no. 11, .
411 <http://dx.doi.org/10.1140/epjc/s10052-012-2205-9>. [2.1.3](#)
- 412 [12] J. C. Collins, D. E. Soper, and G. Sterman, *Factorization for short distance hadron-hadron
413 scattering*, Nuclear Physics B **261** (1985) 104 – 142. [2.2](#)
- 414 [13] CERN, . CERN, Geneva, 1984. [2.2](#)

- 415 [14] LHC Higgs Cross Section Working Group, S. Dittmaier, C. Mariotti, G. Passarino, and
 416 R. Tanaka (Eds.), *Handbook of LHC Higgs Cross Sections: 2. Differential Distributions*,
 417 CERN-2012-002 (CERN, Geneva, 2012) , [arXiv:1201.3084 \[hep-ph\]](https://arxiv.org/abs/1201.3084). 2.2
- 418 [15] *Updated coupling measurements of the Higgs boson with the ATLAS detector using up to 25*
 419 fb^{-1} *of proton-proton collision data*, Tech. Rep. ATLAS-CONF-2014-009, CERN, Geneva, Mar,
 420 2014. 2.2.1
- 421 [16] CMS Collaboration Collaboration, *Precise determination of the mass of the Higgs boson and*
 422 *studies of the compatibility of its couplings with the standard model*, Tech. Rep.
 423 CMS-PAS-HIG-14-009, CERN, Geneva, 2014. 2.2.1
- 424 [17] ATLAS Collaboration Collaboration, G. Aad et al., *Measurement of the Higgs boson mass from*
 425 *the $H \rightarrow \gamma\gamma$ and $H \rightarrow ZZ^* \rightarrow 4l$ channels with the ATLAS detector using 25 fb^{-1} of pp*
 426 *collision data*, [arXiv:1406.3827 \[hep-ex\]](https://arxiv.org/abs/1406.3827). 2.2.1
- 427 [18] *Evidence for the spin-0 nature of the Higgs boson using {ATLAS} data*, Physics Letters B **726**
 428 (2013) no. 13, 120 – 144.
 429 <http://www.sciencedirect.com/science/article/pii/S0370269313006527>. 2.2.1
- 430 [19] S. Dawson, A. Gritsan, H. Logan, J. Qian, C. Tully, et al., *Working Group Report: Higgs*
 431 *Boson*, [arXiv:1310.8361 \[hep-ex\]](https://arxiv.org/abs/1310.8361). 2.2.2
- 432 [20] O. Eberhardt, G. Herbert, H. Lacker, A. Lenz, A. Menzel, et al., *Impact of a Higgs boson at a*
 433 *mass of 126 GeV on the standard model with three and four fermion generations*,
 434 *Phys.Rev.Lett.* **109** (2012) 241802, [arXiv:1209.1101 \[hep-ph\]](https://arxiv.org/abs/1209.1101). 2.2.2
- 435 [21] M. Carena, S. Gori, N. R. Shah, C. E. Wagner, and L.-T. Wang, *Light Stops, Light Staus and*
 436 *the 125 GeV Higgs*, *JHEP* **1308** (2013) 087, [arXiv:1303.4414](https://arxiv.org/abs/1303.4414). 2.2.2
- 437 [22] N. Arkani-Hamed, K. Blum, R. T. D’Agnolo, and J. Fan, *2:1 for Naturalness at the LHC?*,
 438 *JHEP* **1301** (2013) 149, [arXiv:1207.4482 \[hep-ph\]](https://arxiv.org/abs/1207.4482). 2.2.2
- 439 [23] D. Carmi, A. Falkowski, E. Kuflik, and T. Volansky, *Interpreting LHC Higgs Results from*
 440 *Natural New Physics Perspective*, *JHEP* **1207** (2012) 136, [arXiv:1202.3144 \[hep-ph\]](https://arxiv.org/abs/1202.3144). 2.2.2
- 441 [24] G. Degrassi, S. Di Vita, J. Elias-Miro, J. R. Espinosa, G. F. Giudice, et al., *Higgs mass and*
 442 *vacuum stability in the Standard Model at NNLO*, *JHEP* **1208** (2012) 098, [arXiv:1205.6497](https://arxiv.org/abs/1205.6497)
 443 [\[hep-ph\]](https://arxiv.org/abs/1205.6497 [hep-ph]). 2.2.2
- 444 [25] L. Evans and P. Bryant, *LHC Machine*, *JINST* **3** (2008) no. 08, S08001. 3
- 445 [26] T. S. Pettersson and P. Lefevre, *The Large Hadron Collider: conceptual design.*, Tech. Rep.
 446 CERN-AC-95-05 LHC, CERN, Geneva, Oct, 1995. <https://cdsweb.cern.ch/record/291782>.
 447 3
- 448 [27] T. Linnecar et al., *Hardware and Initial Beam Commissioning of the LHC RF Systems.*
 449 *oai:cds.cern.ch:1176380*, Tech. Rep. LHC-PROJECT-Report-1172.
 450 CERN-LHC-PROJECT-Report-1172, CERN, Geneva, Oct, 2008.
 451 <https://cdsweb.cern.ch/record/1176380>. 3
- 452 [28] ATLAS Collaboration, *The ATLAS Experiment at the CERN Large Hadron Collider*, *JINST* **3**
 453 (2008) S08003. 3.1

- 454 [29] The LHCb Collaboration, *The LHCb Detector at the LHC*, Journal of Instrumentation **3** (2008)
455 no. 08, S08005. [3.1](#)
- 456 [30] A. Team, *The four main LHC experiments*, Jun, 1999. [3.1](#)
- 457 [31] ATLAS Collaboration, G. Aad et al., *Improved luminosity determination in pp collisions at \sqrt{s}*
458 $= 7 \text{ TeV using the ATLAS detector at the LHC}$, Eur.Phys.J. **C73** (2013) 2518, arXiv:1302.4393
459 [[hep-ex](#)]. [3.2](#)
- 460 [32] CERN, . CERN, Geneva, 2012. [3.2](#)